N94-22795

# ELECTROMAGNETIC FIELD STRENGTH PREDICTION IN AN URBAN ENVIRONMENT: A USEFUL TOOL FOR THE PLANNING OF LMSS

## G.A.J. van Dooren[1], M.H.A.J. Herben[1], G. Brussaard[1], M. Sforza[2], and J.P.V. Poiares Baptista[2]

[1] Eindhoven University of Technology, Telecommunications Division, PO Box 513,
5600 MB Eindhoven, The Netherlands, tel.:+31-40-473458, fax:+31-40-455197
[2] European Space Technology and Research Centre, Electromagnetics Division, PO Box 299,
2200 AG Noordwijk, The Netherlands, tel.:+31-1719-83298, fax: +31-1719-84999

## ABSTRACT

In this paper a model for the prediction of the electromagnetic field strength in an urban environment is presented. The ray model, that is based on the Uniform Theory of Diffraction (UTD), includes effects of the non-perfect conductivity of the obstacles and their surface roughness. The urban environment is transformed into a list of standardized obstacles that have various shapes and material properties. The model is capable of accurately predicting the field strength in the urban environment by calculating different types of wave contributions such as reflected, edge and corner diffracted waves, and combinations hereof. Also antenna weight functions are introduced to simulate the spatial filtering by the mobile antenna. Communication channel parameters such as signal fading, time delay profiles, Doppler shifts and delay-Doppler spectra can be derived from the ray-tracing procedure using post-processing routines. The model has been tested against results from scaled measurements at 50 GHz and proves to be accurate.

## INTRODUCTION

In the last decade, the market for personal telecommunications is growing rapidly. Therefore, paging channels, mobile, broadcast and portable services have more and more the interest of the planners of modern telecommunications systems. Especially Land Mobile Satellite Systems (LMSS) have a large and continuously increasing interest of system designers and radio wave propagation engineers. It is obvious that, for planning purposes, it is necessary to investigate whether a certain system will meet the required performance criteria *before the system is actually installed.* Therefore, a prediction tool from which information regarding the performance of the communications channel can be deduced, is required. Nowadays, most of the LMSS field prediction models are based on empirical regression fits to numerical measurement results [1, 2, 3] and fail for some particular urban environments. Further, the theoretical models available are often based on crude approximations and assumptions. So a more accurate predictive procedure should use a detailed description of the urban environment in order to analyse the channel characteristics for a number of well defined locations and configurations of the mobile receiver site.

In this paper we describe a deterministic model for field strength prediction in an urban environment, which facilitates the calculation of communication channel parameters such as fading, Doppler shift, and time delay spread. Different types of multipath wave-propagation phenomena, such as reflection, diffraction, and higher order combinations of reflection and/or diffraction, are considered. The model is based on the Uniform Theory of Diffraction (UTD) and includes the effects of the non-perfect conductivity of the obstacles and their surface roughness. Moreover, it permits the antenna characteristics of both the transmitter and receiver to be taken into account. Also, the problem of an object in the near-field of the antennas is addressed and predicted and measured results are compared. Objects with complex shapes are modelled by a number of standardized objects with suitable dimensions and material properties. Particular problems present in conventional prediction methods, such as shadowing and strong specular reflection, are solved by the new model. In this way, our model extends the region of validity of existing models, and improves the physical insight into the wave propagation processes. The major part of this research has been financed by the European Space agency (ESA).

## ELECTROMAGNETIC WAVE MODELLING

The model used to describe the interaction of the incident electromagnetic (EM) wave with the objects in the urban environment is UTD [4], heuristically extended to include effects of non-perfect conductivity and surface roughness [5, 6, 7, 8]. UTD is a high-frequency asymptotic technique that assumes the different waves to propagate along straight lines (rays). This propagation can be mathematically described by:

$$\vec{E}^o = \vec{E}^i \cdot \mathcal{C} \, A(s) \, e^{-jks} \qquad (1)$$

where $\vec{E}^{o,i}$ indicates the outgoing or incident field, $\mathcal{C}$ is a dyadic coefficient describing the physical interaction

of the wave and the object, $A$ is a factor depicting the divergence of the outgoing wave, $k$ is the wavenumber for free space and $s$ is the distance from the observation point to the point on the object at which the interaction took place. The factor $C$ depends on the material properties of the obstacle, the direction of propagation of the incident and outgoing wave, the wavelength and the shape of the obstacle edges and surfaces. Well-known dyadics $C$ are those for LOS (direct) propagation, reflection and diffraction [4] and corner diffraction [9]. Some forms of the divergence factor $A$ are:

$$A(s) = \begin{cases} 1 & \text{, for a plane wave} \\ s^{-1/2} & \text{, for a cylindrical wave} \\ s^{-1} & \text{, for a spherical wave} \end{cases} \quad (2)$$

In our field strength prediction model the following types of waves can be included:

- direct (LOS) wave;
- reflected wave;
- edge diffracted wave;
- reflected-diffracted wave;
- diffracted-reflected wave;
- corner-diffracted wave;
- double-diffracted wave (dd).

Some of the wave contributions are visualized in figure 1. If necessary, contributions of higher order can be taken into account.

Note that the reflection may take place at both the ground and at the obstacle. The reflection and diffraction points can be found using Fermats principle of stationary optical path length [4], yielding reflection points on some face of the obstacle and edge diffraction points at its edges.

Given the coordinates of the source (the satellite) and the observation point (the mobile receiver) and the description of the urban environment, the total field at the observation point can be described by:

$$\begin{aligned} \vec{E}^{obs} \propto \quad & \vec{E}^{LOS} \varepsilon^{LOS} \\ + \quad & \sum_l \vec{E}_l^{refl} \varepsilon_l^{refl} \\ + \quad & \text{other types of rays} \\ + \quad & \sum_m \vec{E}_m^{dd} \varepsilon_m^{dd} \end{aligned} \quad (3)$$

where the functions $\varepsilon$ account for possible blockage of the wave contributions by obstacles in the urban environment.

The received field at the observation point is obtained by first calculating the field strength relative to the free space value (i.e. the case where the field strength is

proportional to the distance between transmitter and receiver). Afterwards the absolute level of the free space value is determined using the well-known radio equation. According to this procedure, the ray-tracing analysis is used to calculate the explicit attenuation of the radio signal induced by the urban environment. This attenuation factor is called site shielding factor (SSF) and is also of interest for other applications [10, 11].

Some of the parameters of interest for the design of a LMSS are the field strength along a trajectory through the urban environment, the mean excess delay time and delay spread, the Doppler spectrum and the delay-Doppler spectrum [12]. These characteristics can be derived by performing a ray-tracing procedure for the environment under consideration and storing the following parameters for each ray and each observation point:

1. the type of ray (LOS, reflected, diffracted, etc.);

2. (complex) $\vec{E}$ vector;

3. direction of propagation;

4. absolute path length measured from source to observation point via the point of stationary phase, or a corner point of the obstacle.

The influence of the antenna receiving pattern of the mobile is simulated by introducing antenna weight functions (in amplitude, phase and polarization). This can be performed *after* the ray tracing for the individual wave contributions has been finished. So, this post-processing feature facilitates the analysis of for instance the antenna type and antenna orientation dependence. The received signal by the antenna is now given by:

$$\begin{aligned} E^{obs} = \quad & \varepsilon^{LOS} G^{LOS} \vec{E}^{LOS} \cdot \hat{e}_{pol}^{LOS} \\ + \quad & \sum_l \varepsilon_l^{refl} G_l^{refl} \vec{E}_l^{refl} \cdot \hat{e}_{pol}^{refl} \\ + \quad & \text{other types of rays} \\ + \quad & \sum_m \varepsilon_m^{dd} G_m^{dd} \vec{E}_m^{dd} \cdot \hat{e}_{pol}^{dd} \end{aligned} \quad (4)$$

where the value of the (complex) antenna voltage patterns $G$ are calculated using the angle between the direction of arrival of the particular ray and boresight direction, while the scalar product with $\hat{e}_{pol}$ accounts for the polarization discrimination.

The post-processor also permits the use of measured antenna patterns by reading the amplitude and phase of a measured antenna voltage pattern from a table. So, different post-processors can provide information on the field strength (co- and cross-polarization), the mean excess delay and delay spread (LOS and obstructed case), and the delay-Doppler spectrum from one and the same ray-tracing file. In this way, the time-consuming

ray-tracing analysis needs to be performed only once for a given observation line and environment.

Note that in some cases an obstacle will be located in the near-field of the antenna or vice-versa. In this particular case it is necessary to consider the combined problem of obstacle and antenna scattering [13]. For ground station reflector antennas this problem has been studied quite extensively and some of the results of this work demonstrate that (theoretically) the combined, near-field method is the only correct approach. For the present application, however, it is decided, both from a computational and a practical point of view, to perform a far-field analysis implying that the interactions of the EM wave with the obstacle and antenna are treated independently.

A time delay analysis is easily performed using the computed data saved for each ray and each observation point. Since each ray will have a different path length from source to observation point, the arrival of the individual waves causes a train of pulses with different amplitudes in the time domain. The same is true in the frequency domain for the Doppler spectrum: each wave will have a different direction of arrival and different amplitude, thereby giving rise to a train of spectral lines in the Doppler spectrum around the carrier frequency. A classification of the arriving waves with respect to the delay time and the Doppler shift will result in the delay-Doppler spectrum [12].

## MODELLING OF URBAN ENVIRONMENT

Since in an urban environment a great variety of obstacle shapes and materials used may occur, there is a need for a flexible, standardized type of obstacle to model the environment.

It was found that therefore the so-called block-shaped obstacle, shown in figure 2, can effectively be used [13]. This obstacle is numerically specified by the (x,y,z) coordinates of its eight corner points. Figure 2 also shows some specific forms of the block-shaped obstacle.

Since it is allowed that some of the corner points (nearly) coalesce, the block-shaped obstacle can effectively be used as an element of a box of building-bricks. Because of this property it is suited to model modern buildings in urban environments (having rectangular shapes) as well as traditional houses in rural environments (having wedge type roof shapes). Also other shapes such as pyramids can easily be modelled and analysed. All combinations of blocks are permitted, and in this way very complex shapes can be built up. Each obstacle has its own material properties and surface roughness. Because of this standardization of obstacle types, only one ray-tracing algorithm is sufficient for the analysis.

The main advantage of the use of the block-type obstacle is the fact that simplifications are introduced

in the calculations of, for example, the reflected and diffracted field parameters. The block-type obstacle has the property that all its sides are straight and all its faces are plane. This implies that phase front of the wave reflected field from one of these planes has the same radii of curvature as that of the incident wave. Because of the straight edges there is no need for the calculation of the caustic distance used in UTD [4].

The modelling proposed has one main disadvantage: cylindrical shapes such as lamp posts and grain warehouses are less accurately modelled. This drawback can be circumvented by approximating a circular cylindrical shape by a combination of two (or more) polygonal cylinders as shown in figure 3. If this approximation appears to be too crude, a second standardized obstacle could be introduced, which possesses a elliptic cylindrical shape. Also this kind of obstacle can be analysed using a UTD theory for convex shapes [14]. It can be shown, however, that the replacement of a cylindrical obstacle by a block-shaped obstacle introduces only considerable changes in the received field *behind* the obstacle. In practice, where a large number of contributions will be received, an error in one of them will lead to just a small error in the whole.

The relevant parameters for the block-type obstacle can be derived semi-automatically from high-accuracy digital databases of rural and urban environments. Also an interface with a CAD package may be developed.

## PRACTICAL VERIFICATION

Recently the model proposed has been experimentally verified for some scaled obstacles at a frequency of 50 GHz [10, 11, 15]. In all comparisons of measurements with theoretical predictions very good agreement has been obtained. Not only the field strength, but also the arrival times of the individual wave contributions were measured and compared to results predicted by the model [10]. From this comparison it was found that the individual rays propagate independently (as assumed in UTD) and that a strong polarization dependence of the signal amplitude exists for conductive block-shaped obstacles [11]. This polarization dependence appears to be due to slope diffraction at the side faces of the obstacle [13] and more or less disappears for less conductive materials [15]. Further, it was found that the corner diffraction contribution can, in some cases, not be neglected in the analysis, especially for low-elevation LMSS.

## ANALYSIS OF TEST CASE

As an illustrative example, we have analysed the 'urban' environment shown in figure 4. The rectangular obstacles have dimensions 86m x 20m x 68m (width x thickness x height), and the pyramid is obtained from

the rectangular block-shaped obstacle by placing the corner points from the top face very close together. Therefore the base of the pyramid is also $86m$ x $20m$ and its height is $68m$. The rectangular building corresponds to the dimensions of the building of Electrical Engineering at the campus of Eindhoven University of Technology. The left rectangular obstacle is assumed to be perfectly conductive and has a surface roughness of 0, the right rectangular obstacle has a relative permittivity $\epsilon_r$ of $2 - 0.1i$ and a surface roughness of $0.1m$, while the pyramid has $\epsilon_r = 3 - 0.2i$ and a surface roughness of $0.1m$. An observation line is defined by the starting point with coordinates $(100m, 75m, 5m)$ and the end point $(-25m, 75m, 5m)$. A total number of 1000 observation points on this line has been used. The satellite position is specified by the azimuth and elevation angles, each having a value of $25°$. The contributions included in the analysis were the direct, reflected, edge diffracted and corner diffracted waves and waves that encounter a combination of reflection and diffraction.

For this geometry we have deduced the field strength on the observation line defined for vertical polarisation at a frequency of 1 GHz and for isotropic transmitting and receiving antennas. This result is shown in figure 5. In this figure the regions of LOS propagation and of strong specular reflection are indicated.

Also the Doppler spectrum around the carrier-frequency of 1 GHz has been calculated for a speed of the mobile of 50 km/h along the trajectory indicated in figure 4. This result is shown in figure 6, where the maximum Doppler shift is 40 Hz. A total of 11500 spectral components are found along the trajectory defined, of which only 10% is plotted in figure 6.

The 3-dimensional delay-Doppler spectrum is shown in figure 7. From this spectrum information on the time delay profile and the Doppler spectrum can be found by using a projection of the data derived onto the time-axis and the Doppler frequency axis, respectively. From a separate time delay analysis it was found that in the LOS regions the mean excess delay time is $0.004\mu s$, while the delay spread is $0.014\mu s$ Further, the mean excess delay time in the obstructed regions is $0.08\mu s$, and the delay spread in these regions is $0.058\mu s$.

These results illustrate the potential of the model developed. The calculations were performed on a 486 computer taking 3 hours of CPU time, resulting in an average of $10s$ per observation point.

## CONCLUSIONS

A deterministic model for the prediction of the field strength in urban environments has been described. The model, that is based on the Uniform Theory of Diffraction (UTD), includes effects of the non-perfect conductivity of the obstacles and their surface roughness. It proves that the use of a flexible, standardized type of obstacle simplifies the ray-tracing algorithms necessary to find reflection and diffraction points. Further, the block-type obstacle proposed is able to (numerically) model frequently encountered shapes such as rectangular blocks (office towers) and wedges (rural rooftops).

The effects of the receiving antenna pattern can be included in a post-processor, which can calculate the field strength along an observation line, together with the Doppler spectrum, time delay profile and the delay-Doppler spectrum. From these parameters relevant information can be deduced for the planning and design of a LMSS.

The model predictions have been verified against scaled measurements at a frequency of 50 GHz. In all cases good agreement between measurements and theory has been obtained.

Besides for mobile communications systems, the model can also be used to analyse the performance indoor radio communications systems. Other fields of technology that may have an interest in the prediction model are (transhorizon) interference prediction, optimal placement of VSAT stations in urban environments, and coupling of interference from terrestrial systems into satellite systems.

# References

[1] Y. Okumura, E. Ohmori, T. Kawano, and K. Fukuda, "Field strength prediction and its variability in VHF and UHF land-mobile radio service", *Rev. Elec. Commun. Lab.*, vol. 16, no. 5, pp. 825–873, 1968.

[2] D.O. Reudink, "Properties of mobile radio propagation above 400 MHz", *IEEE Trans. Veh. Technol.*, vol. VT-23, no. 11, pp. 143–159, 1974.

[3] D.C. Cox, "Multipath delay spread and path loss correlation for 910 MHz urban mobile radio propagation", *IEEE Trans. Veg. Technol.*, vol. VT-26, no. 11, pp. 340–344, 1977.

[4] R.G. Kouyoumjian and P.H. Pathak, "A uniform geometrical theory of diffraction for an edge in a perfectly conducting surface", *Proc. IEEE*, vol. 62, no. 11, pp. 1448–1462, 1974.

[5] R.J. Luebbers, "Propagation prediction for hilly terrain using GTD wedge diffraction", *IEEE Trans. Antennas Propag.*, vol. AP-32, no. 9, pp. 951–955, 1984.

[6] R.J. Luebbers, "Finite conductivity uniform GTD versus knife edge diffraction in prediction of propagation path loss", *IEEE Trans. Antennas Propag.*, vol. AP-32, no. 1, pp. 70–76, 1984.

[7] K.A. Chamberlin and R.J. Luebbers, "An evaluation of Longley-Rice and GTD propagation models", *IEEE Trans. Antennas Propag.*, vol. AP-30, no. 6, pp. 1093–1098, 1982.

[8] R.J. Luebbers, "A heuristic slope diffraction coefficient for rough lossy wedges", *IEEE Trans. Antennas Propag.*, vol. AP-37, no. 2, pp. 206–211, 1989.

[9] F.A. Sikta and W.D. Burnside and T.T. Chu and L.J. Peters JR, "First order equivalent current and corner diffraction scattering from flat plate structures", *IEEE Trans. Antennas Propag.*, vol. AP-31, no. 4, pp. 584–589, 1983.

[10] G.A.J. van Dooren, M.G.J.J. Klaassen, and M.H.A.J. Herben, "Measurement of diffracted electromagnetic fields behind a thin finite-width screen", *Elec. Lett.*, vol. 28, no. 19, pp.1845–1847, 1992.

[11] G.A.J. van Dooren and M.H.A.J. Herben, "Polarization-dependent site-shielding factor of a block-shaped obstacle", *Elec. Lett.*, vol. 29, no. 1, pp. 15–16, 1993.

[12] W.C. Jakes Jr. (editor), *Microwave mobile communications*, New York, John Wiley & sons, 1974.

[13] G.A.J. van Dooren, "Electromagnetic diffraction models for the shielding of single- and dual-reflector antennas by obstacles with simple shapes", IVO Technical Report (ISBN 90-5282-162-3), Eindhoven University of Technology, 1991.

[14] P.H. Pathak, W.D. Burnside, and R.J. Marhefka, "A uniform GTD analysis of the diffraction of electromagnetic waves by a smooth convex surface", *IEEE Trans. Antennas Propag.*, vol. AP-28, no. 5, pp. 631–642, 1980.

[15] G.A.J. van Dooren and M.H.A.J. Herben, "Field strength prediction behind non-perfectly conducting obstacles using UTD", *submitted for publication*, 1993.
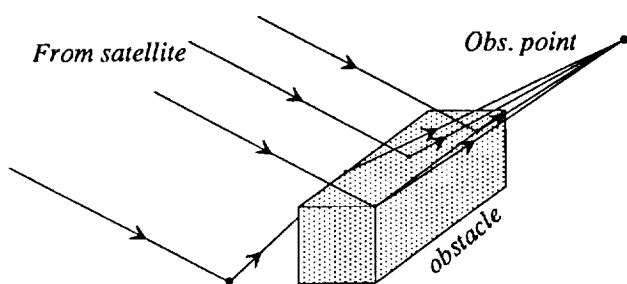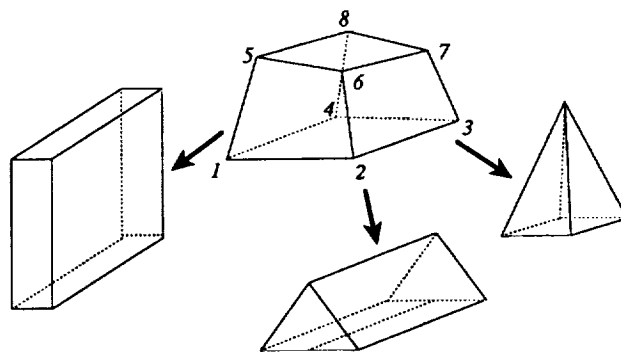
Figure 2: General block-shaped obstacle and some specific obstacles.


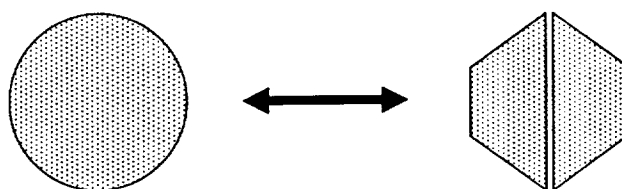
Figure 3: Approximation of a circular cylinder by a combination of polygonal cylinders (a cross section of both shapes is shown).
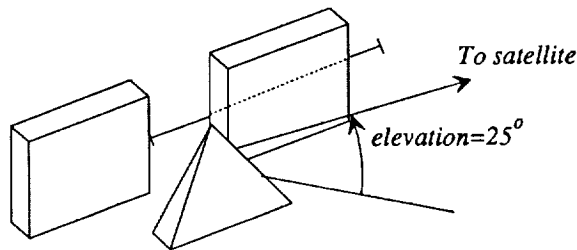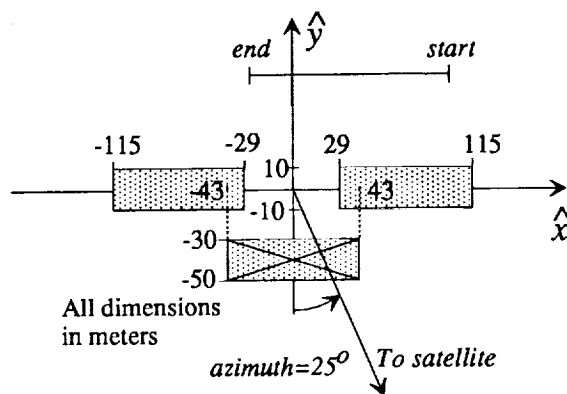


Figure 1: Wave contributions included in the theoretical analysis.



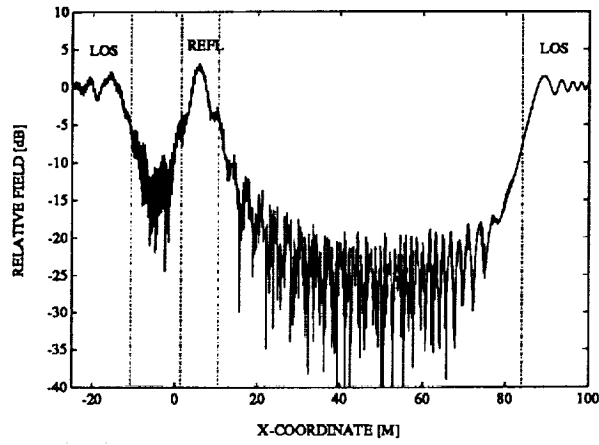Figure 4: Geometrical setup of the testcase.

347

*Figure 5: Calculated field strength along observation line indicated in figure 4.*
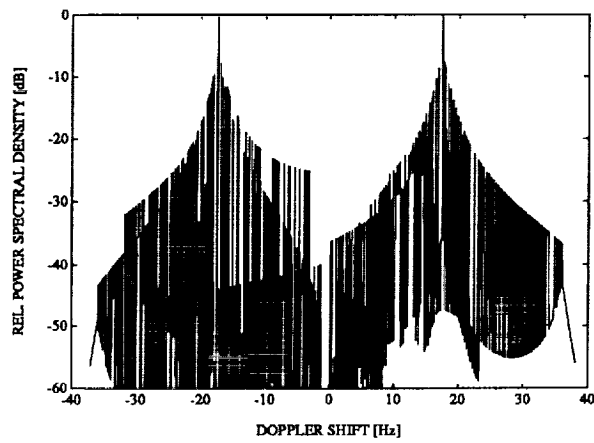


*Figure 6: Calculated Doppler spectrum for observation line indicated in figure 4 at a speed of 50 km/h.*
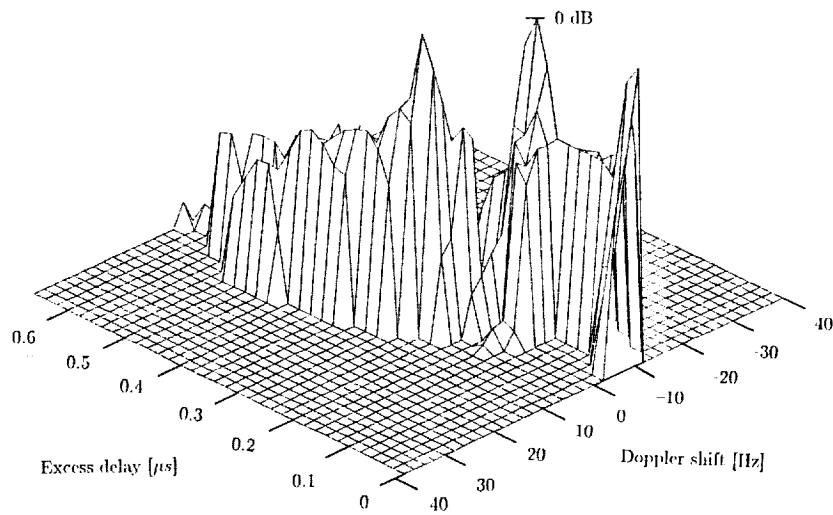


*Figure 7: Calculated delay-Doppler spectrum for observation line indicated in figure 4 at a speed of 50 km/h.*

348